





Emergence of unitary symmetry of microcanonically truncated operators in chaotic quantum systems

Jiaozi Wang ¹, Jonas Richter ^{2,3}, Mats H. Lamann,¹ Robin Steinigeweg ¹, Jochen Gemmer,¹ and Anatoly Dymarsky ⁴

¹*Department of Mathematics/Computer Science/Physics,
University of Osnabrück, D-49076 Osnabrück, Germany*

²*Department of Physics, Stanford University, Stanford, CA 94305, USA*

³*Institut für Theoretische Physik, Leibniz Universität Hannover, 30167 Hannover, Germany*

⁴*Department of Physics, University of Kentucky, Lexington, Kentucky, USA, 40506*
(Dated: June 25, 2024)

We study statistical properties of matrix elements of observables written in the energy eigenbasis and truncated to small microcanonical windows. We present numerical evidence indicating that for all few body operators in chaotic many-body systems, truncated below certain energy scale, collective statistical properties of matrix elements exhibit emergent unitary symmetry. Namely, we show that below certain scale the spectra of the truncated operators exhibit universal behavior, matching our analytic predictions, which are numerically testable for system sizes beyond exact diagonalization. We discuss operator and system-size dependence of the energy scale of emergent unitary symmetry and put our findings in context of previous works exploring emergence of random-matrix behavior at small energy scales.

Introduction. The eigenstate thermalization hypothesis (ETH) [1, 2] provides a microscopic explanation for the emergence of thermodynamic behavior in isolated quantum systems. In the spirit of random-matrix theory, the ETH asserts individual energy eigenstates with similar energies are physically equivalent. Accordingly, matrix elements of observables O_{mn} written in the energy eigenbasis can be described statistically. Qualitatively this leads to a picture where energy eigenstates confined to a sufficiently narrow microcanonical energy window can be randomly reshuffled without changing the statistics of O_{mn} . This picture of ETH based on typicality was advocated in [3–5].

As a stronger statement, parallel to the Bohigas-Giannoni-Schmit conjecture for the energy spectrum [6], for quantum chaotic systems one may expect that matrix elements O_{mn} at sufficiently small scales exhibit full Random-Matrix-Theory universality. A more careful analysis shows that an *uncorrelated*, i.e. Gaussian RMT description, can only apply at very small scales [7–9], as the correlations between matrix elements are inevitable and important to describe various aspects of quantum dynamics [9–13]. An important step is the evidence that O_{mn} can be described by a rotationally invariant ensemble, i.e. general orthogonal or unitary-invariant RMT, that assumes cross-correlations of O_{mn} [14]. In this Letter, we clarify and further establish this picture by first analytically deriving an infinite set of signatures of unitary/orthogonal invariance, and then by testing them numerically. Crucially, we identify relevant energy scale(s) marking the onset of full or partial unitary symmetry. Our numerical approach is based on quantum typicality, and hence applicable to system sizes substantially beyond the reach of exact diagonalization. We confirm that the behavior is consistent with unitary symmetry for all op-

erators in chaotic quantum systems, while for integrable models these signatures are notably absent [15].

Unitary symmetry of microcanonically-truncated operators. We consider an observable O satisfying ETH, with its smooth diagonal part subtracted $\mathcal{O}_{mn} \equiv O_{mn} - O(E)\delta_{mn}$. It is then projected (microcanonically truncated) onto a narrow energy window of width ΔE ,

$$\mathcal{O}_{\Delta E} = P_{\Delta E} O P_{\Delta E}, \quad (1)$$

where we introduce the projector,

$$P_{\Delta E} = \sum_{|E_m - E_0| < \Delta E/2} |E_m\rangle \langle E_m|, \quad (2)$$

and $d = \text{Tr}(P_{\Delta E})$ will denote the number of states within the microcanonical window. We expect that for a sufficiently small scale $\Delta E \leq \Delta E_U$, operator $\mathcal{O}_{\Delta E}$ will exhibit emergent unitary symmetry $U(d)$ [16], which will impose constraints on correlations of the matrix elements as well as on the spectrum of $\mathcal{O}_{\Delta E}$ as a function of ΔE . The idea of studying spectral properties of $\mathcal{O}_{\Delta E}$ in conjunction with their ΔE dependence was put forward in [17], with more detailed studies to follow [7–9, 18–20]. A convenient way to probe the spectrum of the microcanonically truncated operator is through its moments

$$\mathcal{M}_k(\Delta E) = \frac{\text{Tr}[(\mathcal{O}_{\Delta E})^k]}{d(\Delta E)}, \quad (3)$$

which can be combined into free cumulants $\Delta_k = \Delta_k(\Delta E)$ [5], defined through iterative relation

$$\Delta_k = \mathcal{M}_k - \sum_{j=1}^{k-1} \Delta_j \sum_{a_1+a_2+\dots+a_j=k-j} \mathcal{M}_{a_1} \cdots \mathcal{M}_{a_j}. \quad (4)$$

We show in the Supplemental Material [15] that unitary symmetry requires $\Delta_k(\Delta E) \propto (d(\Delta E))^{k-1}$. When ΔE_U is much smaller than the effective temperature, which is always the case for spatially-extended systems, density of states within the microcanonical window is approximately constant, $d(\Delta E)/d(\Delta E_U) = \Delta E/\Delta E_U$, leading to

$$\Delta_k(\Delta E) = \lambda_k \Delta E^{k-1} \quad (5)$$

for $\Delta E \leq \Delta E_U$. Here, Δ_k is a free cumulant of $\mathcal{O}_{\Delta E}$, and λ_k is an operator and system-specific non-universal coefficient. Relations (S19) provide an infinite set of necessary conditions (signatures) of emergent unitary symmetry. We confirm numerically this behavior emerges for all considered operators in a generic nonintegrable quantum spin systems, while also show that in the integrable case this behavior is not present.

In our numerical analysis, we identify ΔE_U with the largest energy window for which (S19) holds for all Δ_k that we are able to compute. More generally, one can define a *cascade* of decreasing scales $\Delta E_U^{(\ell)} \geq \Delta E_U^{(\ell+1)}$, where $\Delta E_U^{(\ell)}$ is defined as the maximal window for which (S19) holds for all $k \leq \ell$. Thus, ΔE_U is identified with $\Delta E_U^{(\ell)}$ for $\ell \rightarrow \infty$.

Emergent unitary symmetry has a clear manifestation at the level of matrix-element correlation functions, captured by the framework of general ETH [5, 21, 22]. The latter proposes that averaged k -th cumulant of \mathcal{O}_{mn} is given by a smooth function f_k of k energies E_i . Emergent unitary symmetry predicts that f_k will be constant [21], which will apply when all E_i are within a narrow energy window of size $\Delta E_U^{(k)}$. For $k=2$ this is the condition that function $f^2(\omega) \equiv f_2(\omega)$ entering the ETH ansatz for $m \neq n$,

$$\mathcal{O}_{mn} = e^{-S/2} f(\omega) r_{mn}, \quad \omega = (E_m - E_n), \quad \overline{r^2} = 1,$$

for $|\omega| \leq \Delta E_U^{(2)}$ is constant. We can readily identify $\Delta E_U^{(2)} \equiv \Delta E_T$ with inverse thermalization timescale of \mathcal{O} , defined as the size of the short-frequency plateau of $f^2(\omega)$. We provide more technical details connecting our results with the framework of general ETH in Supplemental Material [15].

For any $\Delta E \leq \Delta E_U$ unitary symmetry fixes the spectrum of $\mathcal{O}_{\Delta E}$, and the collective statistics of its matrix elements, in terms of the spectrum of $\mathcal{O}_U \equiv \mathcal{O}_{\Delta E_U}$. In particular, for $\Delta E \leq \Delta E_U$, $\mathcal{O}_{\Delta E}$ should in principle admit a description in terms of a rotational-invariant random-matrix model [14], with the parameters of the model fine-tuned to match the spectrum of \mathcal{O}_U . We emphasize, matrix elements within the microcanonical window ΔE_U will show non-trivial correlations constrained only by unitary symmetry. But when truncated to much more narrow windows $\Delta E \ll \Delta E_U$ these correlations will gradually disappear. As follows from (S19), for

$k > 2$, $\Delta_k/\Delta_2^{k/2} \propto (\Delta E/\Delta E_U)^{(k/2-1)} \rightarrow 0$, which implies generic random matrix model reduces to the Gaussian random matrix with uncorrelated \mathcal{O}_{mn} and vanishing cumulants Δ_k . The onset of *Gaussian RMT*, and corresponding scale ΔE_{GUE} , were previously scrutinized numerically in [7–9].

Before embarking on concrete models and numerics, it is natural to ask how ΔE_U would depend on the system size and the type of operator considered. Since the emergent unitary symmetry reshuffles energy *eigenstates*, it is tempting to identify ΔE_U with the Thouless energy scale ΔE_{Th} which marks the onset of random-matrix statistics of energy levels, i.e., emergent unitary symmetry reshuffling energy *eigenvalues*. To complete this proposal, we take into account that Thouless energy controls thermalization time of slowest transport mode present in the system [23–31]. Hence, for a general operator Thouless scale would coincide with inverse thermalization timescale ΔE_T . Given that ω -independence of $\overline{O_{mn}^2}$ is a prerequisite for unitary symmetry, this proposal seems natural. For a generic operator it ties Thouless energy with inverse thermalization time and the scale of unitary symmetry, $\Delta E_{Th} \sim \Delta E_T \equiv \Delta E_U^{(2)} \sim \Delta E_U = \Delta E_U^{(k)}$, $k \rightarrow \infty$.

This picture was first outlined in [3] but it can not be correct in general. As we discussed above, Gaussian random-matrix scale ΔE_{GUE} is expected to be smaller, but *not parametrically* smaller than ΔE_U . At the same time, in one-dimensional systems of length L , ΔE_{GUE} has to be *parametrically* smaller than ΔE_T , specifically $\Delta E_{GUE} \propto \Delta E_T/L$ [9], which contradicts $\Delta E_U \sim \Delta E_T$. This contradiction is further elaborated in Supplemental Material [15], where we provide accurate definitions for all scales. The important point is the cascade of scales

$$\Delta E_{Th} \sim \Delta E_U^{(2)} \geq \dots \geq \Delta E_U^{(k)} \geq \dots \geq \Delta E_U \geq \Delta E_{GUE},$$

with the *parametric* difference between $\Delta E_{Th} \sim \Delta E_U^{(2)}$ and ΔE_U . We leave the question of systematically understanding system-size dependence of $\Delta E_U^{(k)}$ for the future, but note that ΔE_U evaluated numerically below vary significantly for different operators.

Models and Observables. We proceed to study $\Delta_k(\Delta E)$ numerically in a chaotic many-body quantum system, where we consider a one-dimensional Ising model with transverse and longitudinal fields,

$$H = \sum_{\ell=1}^L (g\sigma_x^\ell + h\sigma_z^\ell + J\sigma_z^\ell\sigma_z^{\ell+1}) . \quad (6)$$

$\sigma_{x,z}^\ell$ are Pauli spin operators at site ℓ and periodic boundary conditions are employed, $\sigma_{x,z}^{L+1} \equiv \sigma_{x,z}^1$. We set $J = 1$ and choose the fields as $g = 1$ and $h = 0.5$ for which H is chaotic and expected to fulfill the ETH [32, 33]. To break the translational and reflection symmetries of H , we further add to H two defect terms $h_d\sigma_z^{\lfloor \frac{L}{3} \rfloor}$ and $-h_d\sigma_z^{\lfloor \frac{2L}{3} \rfloor}$

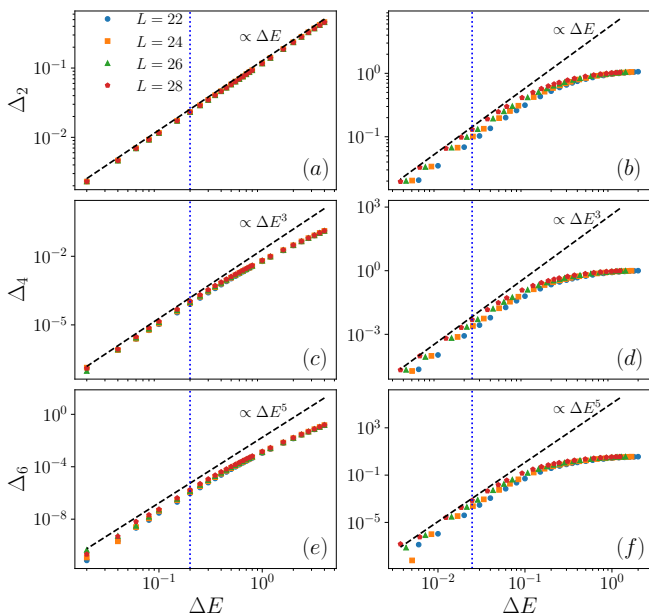


FIG. 1. Even cumulants Δ_k for $k = 2, 4, 6$ as a function of ΔE for the density-wave operator \mathcal{A}_q with the wave-number $q = L/2$ (panels [(a),(c),(e)]) and with $q = 1$ (panels [(b),(d),(f)]). Data are shown for different system sizes $L = 22, 24, 26, 28$. As a guide to the eye, the inclined dashed lines (black) and vertical dotted lines (blue) indicate the theoretically predicted slope $\ln \Delta_k = (k - 1) \ln \Delta E + \text{const}$, and an approximate location of ΔE_U , respectively.

with $h_d = 0.02775$. Our numerical simulations are thus performed in the full Hilbert space of dimension $D = 2^L$. We study density-wave operators of the form,

$$O_q = \frac{1}{\sqrt{L}} \sum_{\ell=1}^L \cos\left(\frac{2\pi}{L} q \ell\right) O^\ell, \quad (7)$$

where we consider different momenta $q = 0, 1, L/2$ and two different local O^ℓ , i.e.,

$$\begin{aligned} \mathcal{A}^\ell &= \frac{h}{2}(\sigma_x^\ell + \sigma_x^{\ell+1}) + \frac{g}{2}(\sigma_z^\ell + \sigma_z^{\ell+1}) + J\sigma_z^\ell \sigma_z^{\ell+1}, \\ \mathcal{B}^\ell &= \frac{g\sigma_z^\ell - h\sigma_x^\ell}{\sqrt{g^2 + h^2}}, \end{aligned} \quad (8)$$

with \mathcal{A}^ℓ being the energy density and \mathcal{B}^ℓ being constructed to have a small overlap with H [17]. Both operators behave in agreement with the usual indicators of the ETH [8, 17] and we denote the corresponding density-wave operators by \mathcal{A}_q and \mathcal{B}_q . Numerical data for the local operators $\mathcal{A}^\ell, \mathcal{B}^\ell$ can be found in [15].

Numerical approach. While studying the properties of $\mathcal{O}_{\Delta E}$ [34] would normally require full exact diagonalization (ED), we can go beyond system sizes accessible to standard ED to compute the moments $\mathcal{M}_k(\Delta E)$ (3).

To evaluate moments, we exploit a pure-state technique based on the concept of quantum typicality [35, 36]

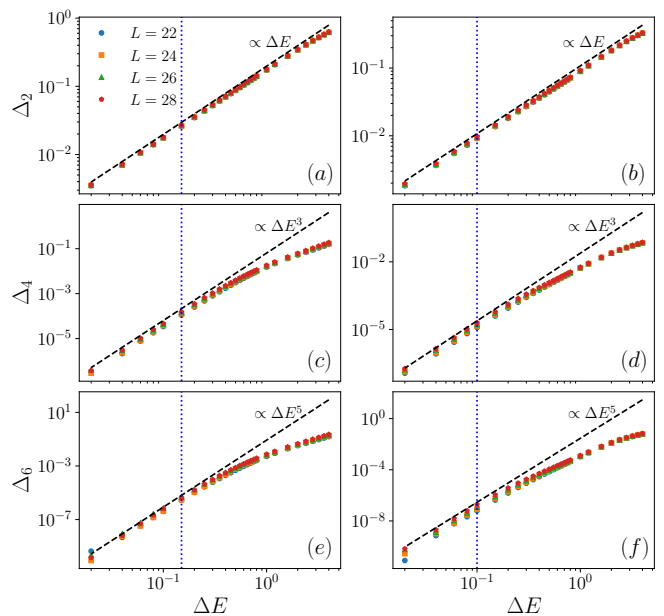


FIG. 2. Similar to Fig. 1, the results for density-wave operator \mathcal{B}_q with $q = \frac{L}{2}$ (panels [(a),(c),(e)]) and $q = 1$ (panels [(b),(d),(f)]).

to compute the moments of $\mathcal{O}_{\Delta E}$ (see also Refs. [8] and [15] for more details). A key idea within this approach is to realize that the energy filter $P_{\Delta E}$ in Eq. (2) can be expanded as [8], $P_{\Delta E} |\psi\rangle \simeq \sum_{i=0}^{N_{\text{tr}}} C_i T_i\left(\frac{H-b}{a}\right) |\psi\rangle$, where $T_i(x)$ are Chebyshev polynomials of the first kind, C_i are appropriately chosen coefficients that encode the energy window ΔE (see [8, 15]), and $a = (E_{\text{max}} - E_{\text{min}})/2$, $b = (E_{\text{max}} + E_{\text{min}})/2$, where $E_{\text{max}(\text{min})}$ are the extremal eigenvalues of H . Moreover, the expansion order N_{tr} has to be chosen large enough to yield accurate results. Given $P_{\Delta E}$, the trace in Eq. (3) can then be approximated by expectation values with respect to random pure states, e.g., for \mathcal{M}_k we have $\mathcal{M}_k \approx \frac{\langle \psi | (P_{\Delta E} \mathcal{O}_{\Delta E})^k | \psi \rangle}{\langle \psi | P_{\Delta E} | \psi \rangle}$, with $|\psi\rangle$ being a Haar-random state constructed in the computational basis. According to quantum typicality, the accuracy of this approximation improves with the number of states d inside the energy window. The accuracy can be further improved by averaging over different realization of random states. By applying $P_{\Delta E}$ efficiently using sparse matrices, we are able to study the free cumulants Δ_k for systems up to $L = 28$.

Results. In Fig. 1, we show cumulants Δ_k as a function of energy window width ΔE , for the energy density-wave operators \mathcal{A}_q for two different wave numbers $q = L/2$ and $q = 1$. Note that for the density-wave operators with $q > 0$ all odd cumulants approximately vanish (for $q = 0$, \mathcal{A}_q is the Hamiltonian apart from the small defect), hence we only show results for even ones $\Delta_{2,4,6}$. In Fig. 1, we observe $\Delta_k \propto \Delta E^{k-1}$ behavior of Eq. (S19) at sufficiently small energy scales, $\Delta E \leq \Delta E_U$, indicating the onset of emergent unitary symmetry. The

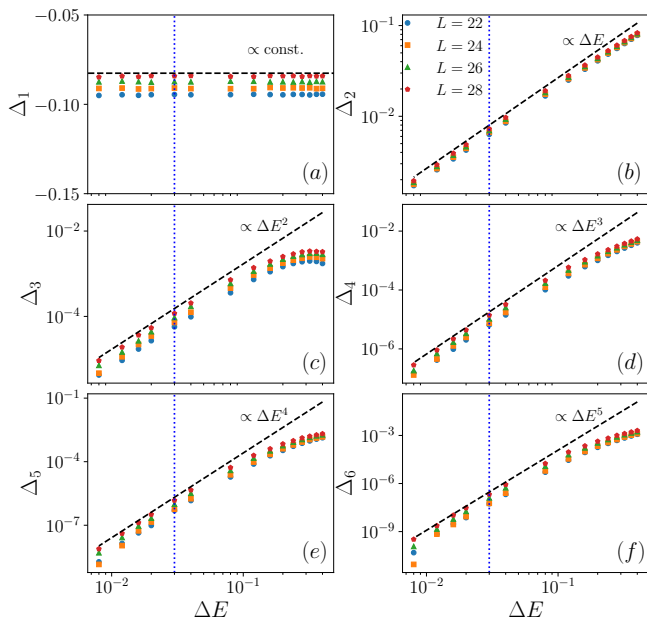


FIG. 3. Similar to Figs. 1, the results for cumulants Δ_k for $k \leq 6$ as a function of ΔE for the density-wave operator \mathcal{B}_q with $q = 0$.

deviations from power-law behavior at extremely small ΔE are due to numerical errors aggravated by small number of states within such energy windows. A very similar picture emerges for the operators \mathcal{B}_q with $q = L/2, 1$ in Fig. 2, with the behavior (S19) clearly visible below certain energy scale. We further observe the predicted power-law behavior for \mathcal{B}_q with $q = 0$ in Fig. 3, where we consider $k \leq 6$ including odd orders. Our results clearly support emergence of unitary symmetry for all operators considered. In the Supplemental material [15], we analyze local operators $\mathcal{A}^\ell, \mathcal{B}^\ell$ and show existence of ΔE_U , and expected power-law behavior below this scale, in these cases as well.

Combined with our theoretical results (S19), Figs. 1 - 3 represent main contribution of this work. Our results demonstrate existence of scale ΔE_U below which the statistical properties of matrix elements \mathcal{O}_{mn} exhibit RMT universality while still admitting non-trivial correlations. Furthermore, scaling behavior (S19), confirmed in Figs. 1 - 3, implies $\Delta_k/(\Delta_2)^{k/2} \rightarrow 0$ when $\Delta E \rightarrow 0$ (up to statistical fluctuations), which confirms that $\mathcal{O}_{\Delta E}$ approaches a Gaussian random matrix at even smaller scales.

Comparing results of Δ_k for different k , we find that in most cases, the size of the energy window marking the onset of $\Delta_k \propto (\Delta E)^{k-1}$ behavior is similar for higher cumulants with $k > 2$, but typically much smaller than the region of linear growth of Δ_2 (the operator \mathcal{A}_1 is an exception, see Fig. 1 (b),(d),(f)). This difference between $\Delta E_U^{(2)}$ and $\Delta E_U^{(k)}$ for $k > 2$ could be related to the fact that correlations between matrix elements have a fingerprint only in higher cumulants $\Delta_{k>2}$. Our data thus sug-

gest that ΔE_U (vertical dashed line in Figs. 1 - 3) in most cases is much smaller than inverse thermalization time $\Delta E_U^{(2)} \equiv \Delta E_T$, tentatively suggesting a scenario when in the thermodynamic limit $\Delta E_U^{(2)} \ll \Delta E_U^{(3)} \sim \dots \sim \Delta E_U$.

A conclusive analysis of L -dependence of $\Delta E_U^{(k)}$ would likely require system sizes much larger than numerically available. Available data in Figs. 1 - 3 (as well as additional data in the Supplemental Material [15]) only indicates that ΔE_U decreases for larger system sizes.

Conclusion & Outlook. In this paper we have introduced a novel energy scale ΔE_U marking the onset of emergent unitary symmetry, i.e., unitary random matrix theory universality of \mathcal{O}_{mn} - matrix elements entering the eigenstate thermalization hypothesis. The scale is operator-specific. For $|E_n - E_m| \leq \Delta E_U$, matrix elements exhibit unitary symmetry, which governs their collective statistical properties. This is to say, below this scale \mathcal{O}_{mn} can be described in terms of a generic RMT. To probe this scale we considered a truncation of an operator \mathcal{O} to microcanonical energy window of size ΔE , defined in (1). We have shown that emergent unitary symmetry for $\Delta E \leq \Delta E_U$ is manifest through a simple power law ΔE dependence of free cumulants Δ_k (4),

$$\Delta_k(\Delta E) \propto (\Delta E)^{k-1}. \quad (9)$$

This provides a set of readily testable criteria, which can be accessed numerically beyond exact diagonalization.

We tested this behavior numerically for different operators satisfying ETH in the case of a generic quantum chaotic spin chain, and in each case found explicit evidence of (9). Corresponding values of ΔE_U marking the onset of this behavior vary significantly for different operators, as well as the ratio $\Delta E_U/\Delta E_T$, where ΔE_T is operator's inverse thermalization time. Our finite-size scaling analysis is not conclusive but consistent with theoretical expectation that in the large system size limit energy scales form the hierarchy $\Delta E_{GUE} \leq \Delta E_U \ll \Delta E_T$, see [15] for details. In particular when $L \rightarrow \infty$, for the considered one-dimensional system we expect both ΔE_{GUE} and ΔE_U to exhibit the same system-size dependence and be parametrically smaller than ΔE_T .

Our results provide a unifying picture, connecting spectral properties of microcanonically-truncated operators [7-9, 17-20] and correlations between off-diagonal matrix elements [10-14, 37-42]. An implicit question underlying these studies is to identify the degree of universality exhibited by the off-diagonal matrix elements of a typical operator in a generic quantum system. An analogous question about universality of energy spectrum of quantum chaotic systems is answered by the famous Bohigas-Giannoni-Schmit conjecture [6], which postulates random matrix universality (with global symmetries of the matrix model matching those of the original system). For the off-diagonal matrix elements, a conceptually similar proposal is given by a general

random matrix theory. The question of universality was recently investigated for holographic models of quantum gravity [40–42], yielding a multi-matrix model description specific for those cases. Our work, which studies a generic quantum chaotic model, provides evidence that emergent unitary symmetry is indeed the universal description for all operators satisfying ETH, with an operator-specific validity range ΔE_U . This picture constitutes a compelling analog of the Bohigas-Giannoni-Schmit conjecture, and deserves further investigation. A natural question would be to repeat our analysis for different types of quantum chaotic systems, including time-dependent Floquet models without energy conservation, as well as semi-classical few-body systems with a chaotic classical counterpart. We also emphasize the question of understanding relative scaling of ΔE_U , ΔE_T and ΔE_{Th} as a key to unite emergent unitary symmetry of this paper with the RMT universality of energy spectrum in one comprehensive framework of quantum chaos.

Acknowledgements. We thank Eugene Kanzieper for extensive discussions concerning random unitary projectors. This work has been funded by the Deutsche Forschungsgemeinschaft (DFG), under Grant No. 531128043, as well as under Grant No. 397107022, No. 397067869, and No. 397082825 within the DFG Research Unit FOR 2692, under Grant No. 355031190. A.D. is supported by the National Science Foundation under Grant No. PHY 2310426. This work was performed in part at Aspen Center for Physics, which is supported by National Science Foundation grant PHY-2210452. J.R. acknowledges funding from the European Union’s Horizon Europe research and innovation programme, Marie Skłodowska-Curie grant no. 101060162, and the Packard Foundation through a Packard Fellowship in Science and Engineering. Additionally, we greatly acknowledge computing time on the HPC3 at the University of Osnabrück, granted by the DFG, under Grant No. 456666331.

[1] J. M. Deutsch, *Quantum statistical mechanics in a closed system*, *Phys. Rev. A* **43**, 2046 (1991).
 [2] M. Srednicki, *Chaos and quantum thermalization*, *Phys. Rev. E* **50**, 888 (1994).
 [3] A. P. Luca D’Alessio, Yariv Kafri and M. Rigol, *From quantum chaos and eigenstate thermalization to statistical mechanics and thermodynamics*, *Advances in Physics* **65**, 239 (2016).
 [4] A. Dymarsky, N. Lashkari, and H. Liu, *Subsystem eigenstate thermalization hypothesis*, *Phys. Rev. E* **97**, 012140 (2018).
 [5] S. Pappalardi, L. Foini, and J. Kurchan, *Eigenstate thermalization hypothesis and free probability*, *Phys. Rev. Lett.* **129**, 170603 (2022).
 [6] O. Bohigas, M.-J. Giannoni, and C. Schmit, *Charac-*

terization of chaotic quantum spectra and universality of level fluctuation laws, *Physical review letters* **52**, 1 (1984).
 [7] J. Richter, A. Dymarsky, R. Steinigeweg, and J. Gemmer, *Eigenstate thermalization hypothesis beyond standard indicators: Emergence of random-matrix behavior at small frequencies*, *Phys. Rev. E* **102**, 042127 (2020).
 [8] J. Wang, M. H. Lamann, J. Richter, R. Steinigeweg, A. Dymarsky, and J. Gemmer, *Eigenstate thermalization hypothesis and its deviations from random-matrix theory beyond the thermalization time*, *Phys. Rev. Lett.* **128**, 180601 (2022).
 [9] A. Dymarsky, *Bound on eigenstate thermalization from transport*, *Phys. Rev. Lett.* **128**, 190601 (2022).
 [10] L. Foini and J. Kurchan, *Eigenstate thermalization hypothesis and out of time order correlators*, *Phys. Rev. E* **99**, 042139 (2019).
 [11] A. Chan, A. De Luca, and J. T. Chalker, *Eigenstate correlations, thermalization, and the butterfly effect*, *Phys. Rev. Lett.* **122**, 220601 (2019).
 [12] C. Murthy and M. Srednicki, *Bounds on chaos from the eigenstate thermalization hypothesis*, *Phys. Rev. Lett.* **123**, 230606 (2019).
 [13] M. Brenes, S. Pappalardi, M. T. Mitchison, J. Goold, and A. Silva, *Out-of-time-order correlations and the fine structure of eigenstate thermalization*, *Phys. Rev. E* **104**, 034120 (2021).
 [14] L. Foini and J. Kurchan, *Eigenstate thermalization and rotational invariance in ergodic quantum systems*, *Phys. Rev. Lett.* **123**, 260601 (2019).
 [15] See supplemental material for the derivation of Eq. (S19), definition of λ_k , additional numerical results, rigorous definition of different energy scales, discussions on unitary symmetry in integrable case and details on our numerical approach. Supplemental material includes Refs. [43–48].
 [16] Unitary symmetry can be understood as rotational invariance of the probability measure $P(\mathcal{O}_{mn}) = P(\mathcal{O}'_{mn})$, $\mathcal{O}' = U\mathcal{O}U^\dagger$. The type of symmetry depends on global symmetries of H and O . When both exhibit time-reversal symmetry, *unitary* symmetry $U(d)$ should be substituted by *orthogonal* symmetry. Nevertheless we use the notations ΔE_U (and ΔE_{GUE} for corresponding Gaussian ensemble) throughout the paper for the scales marking the onset of corresponding regimes.
 [17] A. Dymarsky and H. Liu, *New characteristic of quantum many-body chaotic systems*, *Phys. Rev. E* **99**, 010102 (2019).
 [18] A. Dymarsky, *Mechanism of macroscopic equilibration of isolated quantum systems*, *Phys. Rev. B* **99**, 224302 (2019).
 [19] S. Pappalardi, L. Foini, and J. Kurchan, *Microcanonical windows on quantum operators*, *Quantum* **8**, 1227 (2024).
 [20] F. Iniguez and M. Srednicki, *Microcanonical truncations of observables in quantum chaotic systems*, arXiv preprint arXiv:2305.15702 (2023).
 [21] S. Pappalardi, F. Fritzsche, and T. Prosen, *General eigenstate thermalization via free cumulants in quantum lattice systems*, arXiv preprint arXiv:2303.00713 (2023).
 [22] M. Fava, J. Kurchan, and S. Pappalardi, *Designs via free probability*, arXiv preprint arXiv:2308.06200 (2023).
 [23] B. Altshuler and B. Shklovskii, *Repulsion of energy levels and conductivity of small metal samples*, *Sov. Phys. JETP* **64**, 127 (1986).

- [24] A. J. Friedman, A. Chan, A. De Luca, and J. T. Chalker, *Spectral statistics and many-body quantum chaos with conserved charge*, *Phys. Rev. Lett.* **123**, 210603 (2019).
- [25] M. Winer and B. Swingle, *Hydrodynamic theory of the connected spectral form factor*, *Phys. Rev. X* **12**, 021009 (2022).
- [26] M. Winer and B. Swingle, *Spontaneous symmetry breaking, spectral statistics, and the ramp*, *Phys. Rev. B* **105**, 104509 (2022).
- [27] M. Winer and B. Swingle, *Emergent spectral form factors in sonic systems*, *Phys. Rev. B* **108**, 054523 (2023).
- [28] M. Winer and B. Swingle, *Reappearance of thermalization dynamics in the late-time spectral form factor*, arXiv preprint arXiv:2307.14415 (2023).
- [29] D. Roy and T. c. v. Prosen, *Random matrix spectral form factor in kicked interacting fermionic chains*, *Phys. Rev. E* **102**, 060202 (2020).
- [30] D. Roy, D. Mishra, and T. c. v. Prosen, *Spectral form factor in a minimal bosonic model of many-body quantum chaos*, *Phys. Rev. E* **106**, 024208 (2022).
- [31] V. Kumar and D. Roy, *Many-body quantum chaos in mixtures of multiple species*, *Phys. Rev. E* **109**, L032201 (2024).
- [32] M. C. Bañuls, J. I. Cirac, and M. B. Hastings, *Strong and weak thermalization of infinite nonintegrable quantum systems*, *Phys. Rev. Lett.* **106**, 050405 (2011).
- [33] J. F. Rodriguez-Nieva, C. Jonay, and V. Khemani, *Quantifying quantum chaos through micro-canonical distributions of entanglement*, arXiv preprint arXiv:2305.11940 (2023).
- [34] Although in principle one needs to consider an operator O with its smooth diagonal part (in the energy eigenbasis) subtracted, for small ΔE , the contribution of the non-trivial part of $O(E)\delta_{mn}$ to the cumulants Δ_k will be suppressed by the system size. Thus, in our numerical analysis we use the original observable O .
- [35] T. Heitmann, J. Richter, D. Schubert, and R. Steinigeweg, *Selected applications of typicality to real-time dynamics of quantum many-body systems*, *Zeitschrift für Naturforschung A* **75**, 421 (2020).
- [36] F. Jin, D. Willsch, M. Willsch, H. Lagemann, K. Michielsen, and H. De Raedt, *Random state technology*, *Journal of the Physical Society of Japan* **90**, 012001 (2021).
- [37] D. Hahn, D. J. Luitz, and J. Chalker, *The statistical properties of eigenstates in chaotic many-body quantum systems*, arXiv preprint arXiv:2309.12982 (2023).
- [38] A. Belin, J. de Boer, and D. Liska, *Non-gaussianities in the statistical distribution of heavy ope coefficients and wormholes*, *Journal of High Energy Physics* **2022**, 1 (2022).
- [39] T. Anous, A. Belin, J. de Boer, and D. Liska, *Ope statistics from higher-point crossing*, *Journal of High Energy Physics* **2022**, 1 (2022).
- [40] D. L. Jafferis, D. K. Kolchmeyer, B. Mukhametzhanov, and J. Sonner, *Matrix models for eigenstate thermalization*, *Phys. Rev. X* **13**, 031033 (2023).
- [41] D. L. Jafferis, D. K. Kolchmeyer, B. Mukhametzhanov, and J. Sonner, *Jackiw-teitelboim gravity with matter, generalized eigenstate thermalization hypothesis, and random matrices*, *Phys. Rev. D* **108**, 066015 (2023).
- [42] A. Belin, J. de Boer, D. L. Jafferis, P. Nayak, and J. Sonner, *Approximate cfts and random tensor models*, arXiv preprint arXiv:2308.03829 (2023).
- [43] P. J. Forrester, *Quantum conductance problems and the jacobi ensemble*, *Journal of Physics A: Mathematical and General* **39**, 6861 (2006).
- [44] D. V. Savin, H.-J. Sommers, and W. Wieczorek, *Non-linear statistics of quantum transport in chaotic cavities*, *Phys. Rev. B* **77**, 125332 (2008).
- [45] P. Vidal and E. Kanzieper, *Statistics of reflection eigenvalues in chaotic cavities with nonideal leads*, *Phys. Rev. Lett.* **108**, 206806 (2012).
- [46] Z. Puchala and J. Miszczyk, *Symbolic integration with respect to the haar measure on the unitary groups*, *Bulletin of the Polish Academy of Sciences Technical Sciences* **65**, 21 (2017).
- [47] A. Weiße, G. Wellein, A. Alvermann, and H. Fehske, *The kernel polynomial method*, *Rev. Mod. Phys.* **78**, 275 (2006).
- [48] J. C. Osborn and J. J. M. Verbaarschot, *Thouless energy and correlations of qcd dirac eigenvalues*, *Phys. Rev. Lett.* **81**, 268 (1998).
- [49] M. Srednicki, *The approach to thermal equilibrium in quantized chaotic systems*, *Journal of Physics A: Mathematical and General* **32**, 1163 (1999).

SUPPLEMENTAL MATERIAL

Random unitary projector

Our starting point is a large $N \times N$ matrix A (with $N \gg 1$), projected onto an M -dimensional subspace with a Haar-random unitary projector. We can write that explicitly as

$$\tilde{A} = P U A U^\dagger P^T, \quad (\text{S1})$$

where U is an $N \times N$ Haar-random unitary and P is a fixed projector of rank M , an $M \times N$ matrix satisfying $PP^T = \mathcal{I}_M$. Although not necessary for what follows, we can introduce an $M \times M$ Haar-random unitary V with the substitution $P \rightarrow VP$, such that resulting $M \times M$ matrix \tilde{A} will exhibit unitary symmetry, and the spectrum will be its only invariant. The combination $VP U$ is a random unitary projector.

For simplicity we can choose P to be the projector on first M coordinates

$$\tilde{A}_{ij} = U_i^k A_{kl} (U^*)_j^l, \quad 1 \leq i, j \leq M, \quad 1 \leq k, l \leq N. \quad (\text{S2})$$

At this point it is convenient to use block representation of the Haar-random unitary (orthogonal) matrix U , which is well-known in physics literature modeling scattering matrix of 1D systems [43–45],

$$U = \left(\begin{array}{c|c} r_{M \times M} & t_{M \times (N-M)} \\ \hline t'_{(N-M) \times M} & r'_{(N-M) \times (N-M)} \end{array} \right), \quad (\text{S3})$$

Here,

$$\begin{aligned} r_{M \times M} &= u_1 \text{diag}(1 - T_i) u_2^\dagger, & (\text{S4}) \\ t_{M \times (N-M)} &= i u_1 \Lambda v_2^\dagger, & \Lambda_{ij} = \delta_{ij} T_i^{1/2}, & (\text{S5}) \end{aligned}$$

where u_1, u_2 are two Haar-random $M \times M$ unitary matrices and v_1, v_2 are two random $(N - M) \times (N - M)$ unitary matrices. Moreover, $T_i = 0$ for $i > M$, while for $i \leq M$, $0 \leq T_i \leq 1$ are random variables with a joint probability distribution,

$$dP = \frac{1}{S} \prod_{i=1}^M dT_i T_i^{\alpha-1} \prod_{i < j} |T_i - T_j|^\beta, \quad (\text{S6})$$

with $\alpha = \beta(N - 2M + 1)/2$, and $\beta = 1, 2, 4$ as usual marks GOE, GUE, or GSE ensemble (meaning U and other matrices above may have been Haar-orthogonal or Haar-symplectic). Above we have also assumed that $M \leq N/2$. Factor S in (S6) is added for normalization, it can be evaluated explicitly using Selberg integral,

$$\begin{aligned} S(\tilde{\alpha}, \tilde{\beta}, \tilde{\gamma}) &= \prod_{i=1}^M dT_i T_i^{\tilde{\alpha}-1} (1 - T_i)^{\tilde{\beta}-1} \prod_{i < j} |T_i - T_j|^{2\tilde{\gamma}} \\ &= \prod_{j=0}^{M-1} \frac{\Gamma(\tilde{\alpha} + j\tilde{\gamma}) \Gamma(\tilde{\beta} + j\tilde{\gamma}) \Gamma(1 + (j+1)\tilde{\gamma})}{\Gamma(\tilde{\alpha} + \tilde{\beta} + (M+j-1)\tilde{\gamma}) \Gamma(1 + \tilde{\gamma})}, \end{aligned}$$

with the parameters $\tilde{\alpha} = \alpha$, $\tilde{\beta} = 1$, $\tilde{\gamma} = \beta/2$. The expectation value of the product $T_1 T_2 \dots T_k$ with the measure (S6) is given by Aomoto's integral formula,

$$\begin{aligned} &\prod_{i=1}^M dT_i T_i^{\tilde{\alpha}-1} \left(\prod_{i=1}^k T_i \right) (1 - T_i)^{\tilde{\beta}-1} \prod_{i < j} |T_i - T_j|^{2\tilde{\gamma}} \\ &= S \prod_{j=1}^k \frac{\tilde{\alpha} + (M-j)\tilde{\gamma}}{\tilde{\alpha} + \tilde{\beta} + (2M-j-1)\tilde{\gamma}}. \end{aligned} \quad (\text{S7})$$

After changing the variables $T_i \rightarrow 1 - T_i$ we find,

$$\left\langle \prod_{i=1}^k (1 - T_i) \right\rangle = \frac{\tilde{M}! (\tilde{N} - k)!}{\tilde{N}! (\tilde{M} - k)!}, \quad (\text{S8})$$

where $\tilde{M} = M + 2/\beta - 1$, and $\tilde{N} = N + 2/\beta - 1$. Since we are working in the limit of large $N \geq M \gg 1$ the difference between \tilde{M}, \tilde{N} and M, N and hence the difference between different Gaussian ensembles (unitary, orthogonal or symplectic) can be neglected. Our goal is to evaluate moments of \tilde{A}

$$\mathcal{M}_k = \frac{\langle \text{Tr} \tilde{A}^k \rangle}{M}, \quad (\text{S9})$$

starting from the known moments of A , $\mathcal{A}_k = \text{Tr}(A^k)/N$. As a starting point we evaluate,

$$\det(z - \tilde{A}) = z^M e^{\text{Tr} \ln(1 - \tilde{A}/z)}. \quad (\text{S10})$$

Without loss of generality we can assume matrix A is diagonal, with the eigenvalues a_i . Furthermore, as a technical assumption, we consider the case when all $a_i = 0$ for $i > M$. It is easy to see then that each term in $1/z$ expansion of

$$\begin{aligned} e^{\text{Tr} \ln(1 - \tilde{A}/z)} &= \\ 1 - \frac{\sum_i (1 - T_i) a_i}{z} + \frac{\sum_{i \neq j} (1 - T_i)(1 - T_j) a_i a_j / 2}{z^2} + \dots \end{aligned} \quad (\text{S11})$$

only involve products of $1 - T_i$ with distinct indexes. Using (S8) we readily find,

$$\langle \det(z - \tilde{A}) \rangle = z^M \sum_{k=0}^{\infty} \frac{a_k}{z^k} \frac{\tilde{M}! (\tilde{N} - k)!}{\tilde{N}! (\tilde{M} - k)!}, \quad (\text{S12})$$

where a_k are defined via,

$$\begin{aligned} \exp \left(- \sum_{k=1}^{\infty} \frac{\text{Tr}(A^k)}{k z^k} \right) &\equiv 1 + \sum_{k=1}^{\infty} \frac{a_k}{z^k}, & (\text{S13}) \\ a_1 &= -\text{Tr} A, & a_2 &= \frac{(\text{Tr} A)^2 - \text{Tr} A^2}{2}, \quad \dots \end{aligned}$$

Eventually, we are interested in calculating resolvent

$$\frac{1}{M} \left\langle \text{Tr} \frac{1}{z - \tilde{A}} \right\rangle = \frac{1}{z} + \sum_{k=1}^{\infty} \frac{\mathcal{M}_k}{z^{k+1}}, \quad (\text{S14})$$

which is given by z -derivative of $\langle \ln \det(z - \tilde{A}) \rangle$. In the large- M limit we can instead evaluate z -derivative of $\ln \langle \det(z - \hat{A}) \rangle$ yielding,

$$\sum_{k=1}^{\infty} \frac{\mathcal{M}_k}{z^{k+1}} = \frac{1}{M} \frac{d}{dz} \ln \left(1 + \sum_{k=1}^{\infty} \frac{a_k}{z^k} \frac{M!(N-k)!}{N!(M-k)!} \right).$$

We have removed tilde from M and N because we are working in the large- M, N limit. After introducing $\alpha = M/N$ in the large- M, N limit we find

$$\begin{aligned} \mathcal{M}_1 &= \mathcal{A}_1, \\ \mathcal{M}_2 &= \alpha \mathcal{A}_2 + (1 - \alpha) \mathcal{A}_1^2, \\ \mathcal{M}_3 &= \alpha^2 \mathcal{A}_3 + 3\alpha(1 - \alpha) \mathcal{A}_1 \mathcal{A}_2 + (2\alpha^2 - 3\alpha + 1) \mathcal{A}_1^3, \\ \mathcal{M}_4 &= \alpha^3 \mathcal{A}_4 + 4\alpha^2(1 - \alpha) \mathcal{A}_1 \mathcal{A}_3 + 2\alpha^2(1 - \alpha) \mathcal{A}_2^2 + \\ &\quad 2\alpha(5\alpha^2 - 8\alpha + 3) \mathcal{A}_1^2 \mathcal{A}_2 + (-5\alpha^3 + 10\alpha^2 - 6\alpha + 1) \mathcal{A}_1^4, \\ &\dots, \end{aligned} \quad (\text{S15})$$

c.f. Eqs. (7) and (8) in the main text. Here we have dropped the assumption that A has at most M non-zero eigenvalues. Correctness of final result can be checked for low moments directly by writing it in components, e.g.,

$$M \mathcal{M}_2 = \sum_{i,j=1}^M \sum_{k,l,r,t=1}^N \langle U_{ik} A_{kl} U_{lj}^* U_{jr} A_{rt} U_{ti}^* \rangle, \quad (\text{S16})$$

and using multi-point correlations of individual matrix elements U_{ij} [46]. At this point we introduce free cumulants Δ_k

$$\begin{aligned} \Delta_1 &= \mathcal{M}_1 \\ \Delta_2 &= \mathcal{M}_2 - \mathcal{M}_1^2 \\ \Delta_3 &= \mathcal{M}_3 - 3\mathcal{M}_2 \mathcal{M}_1 + 2\mathcal{M}_1^3 \\ \Delta_4 &= \mathcal{M}_4 - 4\mathcal{M}_3 \mathcal{M}_1 - 2\mathcal{M}_2^2 + 10\mathcal{M}_2 \mathcal{M}_1^2 - 5\mathcal{M}_1^4 \\ &\vdots \end{aligned} \quad (\text{S17})$$

After a straightforward calculation Eq. (S15) yields

$$\Delta_k^{(M)} = \alpha^{k-1} \Delta_k^{(N)}, \quad (\text{S18})$$

where $\Delta_k^{(M)}$ and $\Delta_k^{(N)}$ indicate free cumulants defined in terms of moments \mathcal{M} and \mathcal{A} , respectively. Eq. (S18) implies a universal behavior of free cumulants under unitary symmetry.

We provide a numerical check of our analytical result, Eq. (S18). To that end we consider a diagonal random matrix \mathcal{O}^* from Eq. (5) in the main text, with the matrix elements drawn from the 4th order χ^2 distribution, and the transformation U from a Haar-random orthogonal ensemble (one can think of a Hamiltonian drawn from the GOE). We evaluate free cumulants Δ_k numerically and show them as a function of the ratio $\alpha = \frac{d}{D}$ (ratio of the energy window's dimension and the whole Hilbert

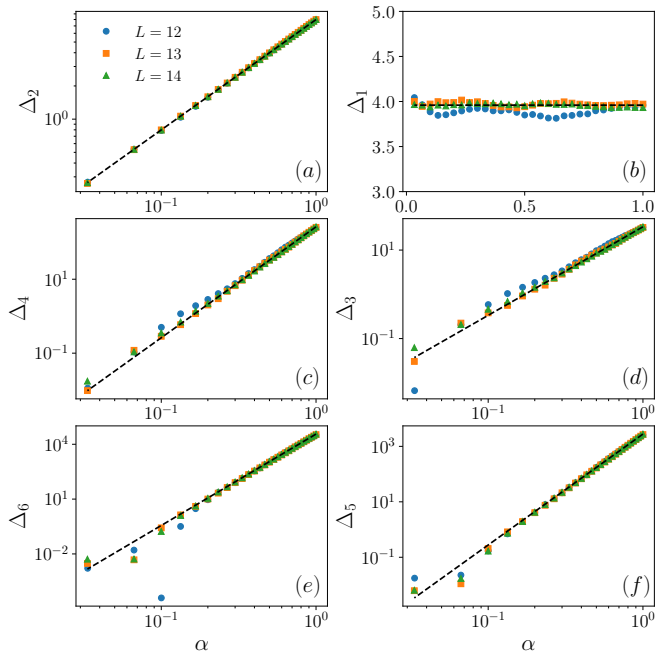


FIG. S1. Numerical demonstration of the analytic results for a random-matrix toy model. Free cumulants Δ_k versus $\alpha = \frac{d}{D}$ for an operator \mathcal{O} whose spectrum follows a 4th order χ^2 distribution and a Hamiltonian drawn from GOE, leading to the Haar-random orthogonal U . Results are shown for Hilbert-space dimension $D = 2^L$, where $L = 12, 13, 14$. As a guide to the eye, the dashed line indicates the theoretically predicted slope $\ln \Delta_k = (k - 1) \ln d + \text{const}$.

space size) in Fig. S1. The scaling $\Delta_k \propto \alpha^{k-1}$ can be clearly observed, except for the fluctuations at the very small window sizes, which are due to insufficient statistics for very small d . The results are in agreement with (S18).

If we now assume that microcanonically projected operator $\mathcal{O}_{\Delta E}$ from the main text, for $\Delta E \leq \Delta E_U$ exhibits (emergent) unitary symmetry, and assuming ΔE_U is small enough such that density of states is approximately constant $d(\Delta E) \propto \Delta E$, we find

$$\Delta_k(\Delta E) = \lambda_k \Delta E^{k-1}, \quad (\text{S19})$$

where $\lambda_k = \Delta_k^U / (\Delta E_U)^{k-1}$, Δ_k^U are k -th cumulants of $\mathcal{O}_U \equiv \mathcal{O}_{\Delta E_U}$.

Relation to general ETH

We consider the same theoretical model as above, a unitary-invariant operator

$$\mathcal{O}_U = U \mathcal{O}^* U^\dagger, \quad (\text{S20})$$

where U is a Haar-random unitary operator of size $d_U \equiv d(\Delta E_U)$. We denote the matrix elements of \mathcal{O}_U simply by \mathcal{O}_{ij} (subindex U is dropped), and study correlation

functions between matrix elements,

$$F_k(i_1, \dots, i_k) := \overline{\mathcal{O}_{i_1 i_2} \cdots \mathcal{O}_{i_k i_1}}, \quad (\text{S21})$$

where averaging is over the unitary group. One can readily see that the result is independent of i_1, \dots, i_k

$$F_k = d_U^{k-1} \Delta_k^U, \quad (\text{S22})$$

where Δ_k^U is the k -th free cumulant of \mathcal{O}_U . To make a connection with general ETH, we consider an operator \mathcal{O}_{mn} written in the eigenbasis of a chaotic Hamiltonian H . Then the correlation function,

$$\overline{\mathcal{O}_{i_1 i_2} \cdots \mathcal{O}_{i_k i_1}} = e^{-(k-1)S(E_+)} f_k(\vec{\omega}), \quad (\text{S23})$$

where average is understood to be over the values of i_α within some narrow intervals centered around E_α , will be a smooth function of its arguments,

$$E_+ = (E_1 + \cdots + E_k)/k, \quad (\text{S24})$$

$$\vec{\omega} = (E_2 - E_1, \dots, E_k - E_{k-1}), \quad (\text{S25})$$

This was recently proposed and verified numerically in [5, 21].

Comparing this with the prediction of unitary invariant model above, we readily conclude that emergent unitary symmetry at scales smaller than ΔE_U is equivalent to condition that cumulants $f_k(\vec{\omega})$ become constant at small frequencies, when all components of $\vec{\omega}$ are not exceeding ΔE_U ,

$$f_k(\vec{\omega}) = (e^{S(E_+)}/d_U)^{k-1} \Delta_k^U. \quad (\text{S26})$$

Taking into account Eq. (9) in the main text, this expression will not change if instead of ΔE_U one considers any other smaller window $\Delta E < \Delta E_U$.

For example for $k = 2$ we find,

$$f^2(\bar{E}, \omega) = (e^{S(\bar{E})}/d)\Delta_2, \quad \text{for } |\omega| \leq \Delta E_U, \quad (\text{S27})$$

in full agreement with the ETH ansatz [49],

$$\mathcal{O}_{mn} = \mathcal{O}(\bar{E})\delta_{mn} + e^{-\frac{S(\bar{E})}{2}} f(\bar{E}, \omega) r_{mn}, \quad (\text{S28})$$

$$\omega = E_m - E_n, \quad \bar{E} = (E_m + E_n)/2. \quad (\text{S29})$$

We emphasize, constant value of $f^2(\omega)$ is a necessary but not sufficient condition for unitary symmetry. Full unitary symmetry requires all higher cumulant functions f_k to be constant at small frequencies, when all components of $\vec{\omega}$ are smaller than ΔE_U . This condition was already recognized in [5, 21] as the condition for the ‘‘rotation-invariant ETH’’ of [14], which, up to certain subtleties, is mathematically equivalent to the model we considered. The crucial difference between our work and [5, 14, 21] is in the choice of observables and the numerical method, which allows us to probe the scale when this behavior emerge. Evaluating cumulant functions f_k requires exact

diagonalization, which limits analysis to modest system sizes. By formulating the implications of unitary symmetry in terms of cumulants Δ_k we devised the readily testable predictions (Eq. (9) in the main text), which can be probed numerically at larger system sizes with help of methods of typicality.

Definitions and the relation between $\Delta_{E_{Th}}, \Delta_{E_T}, \Delta_{E_U}, \Delta_{E_{GUE}}$

We start with Thouless energy $\Delta_{E_{Th}}$, which marks the onset of Random Matrix Theory behavior of energy levels. To define $\Delta_{E_{Th}}$ one considers *level rigidity*, variance in the number N of energy levels within a narrow micro-canonical window of width ΔE , centered around some E ,

$$(\langle N^2 \rangle - \langle N \rangle^2)(\Delta E). \quad (\text{S30})$$

Averaging here is understood in terms of choosing different windows, with different but similar central energy E , with the same energy density.

For a quantum chaotic system the Bohigas-Giannoni-Schmit conjecture [6] predicts that for sufficiently small ΔE the answer of level rigidity would be the same as given by a Gaussian RMT. Say, in case of GUE, the variance would be proportional to $\ln(\Delta E)$. Thouless energy is defined as the smallest ΔE , for which variance will start deviating from the RMT value. To quantify that, one normally introduces a small parameter ϵ , such that

$$\left| \frac{\langle N^2 \rangle_{RMT}}{\langle N^2 \rangle} - 1 \right|_{\Delta E_{Th}} = \epsilon. \quad (\text{S31})$$

A similar definition can be given in time domain in terms of the spectral form factor.

For spatially-extended systems with local interaction Thouless energy will be decreasing (non increasing) with system size, while the density of states e^S will be a function of energy density E/V , where V is the volume. Thus, for sufficiently large systems the definition of $\Delta_{E_{Th}}$ would not require spectrum unfolding, which is a standard numerical procedure to define $\Delta_{E_{Th}}$ for finite V [48].

The definition above is ambiguous, it depends on an arbitrary small parameter ϵ . The idea is to keep ϵ fixed while taking system size V to be very large. In this case $\Delta_{E_{Th}}$ defines a *scale*, together with its system-size dependence. It is expected that the inverse Thouless energy $1/\Delta_{E_{Th}}$ will be the timescale of the slowest transport mode [23–28]. For a chaotic 1D system of the kind discussed in the main text, we expect the slowest transport mode to be diffusive, yielding $\Delta_{E_{Th}} \sim L^{-2}$, where L is the system length.

Next we discuss inverse thermalization time E_T . Unlike $\Delta_{E_{Th}}$, which was a property of Hamiltonian, inverse

thermalization time, as well as scales ΔE_U and ΔE_{GUE} introduced below, are operator-specific. We define E_T as an inverse thermalization time, where the latter is time T which marks the saturation of the (integral of the) 2pt-function of \mathcal{O} . In the energy domain this is the same as the size of the plateau region of f^2 (S28) at small ω . In practice to define E_T we use free cumulant $\Delta_2(\Delta E)$. As discussed above, constant $f^2(\omega)$ is equivalent to linearly growing $\Delta_2(\Delta E)$, we thus define ΔE_T as the minimal value of ΔE for which Δ_2 deviates from linear growth

$$\left| \frac{\Delta_2}{a \Delta E} - 1 \right|_{\Delta E_T} = \epsilon, \quad (\text{S32})$$

and $a \Delta E$ is the best fit for $\Delta_2(\Delta E)$ at small ΔE .

As in the case of Thouless energy we had to introduce an arbitrary small parameter ϵ [not related to ϵ in (S31)], and assume that system size V is very large, such that one can neglect nonlinearities of the energy spectrum density. This definition provides a rigorous way, at least in principle, to define ΔE_T scaling with V . As we mentioned before, it is expected that ΔE_{T_h} will match ΔE_T for the slowest operator (i.e. smallest ΔE_T among all local operators) in the sense of system-size dependence, $E_{T_h} \sim E_T$. Thus, for the spin chain discussed in the text, which we expect to be diffusive, for typical local operators we expect $E_T \sim L^{-2}$. For the density-wave operators (Eq. (11) in the main text) we expect

$$\Delta E_T \sim \frac{q^2}{L^2}, \quad (\text{S33})$$

where q controls the wave length. Our numerical data is too sensitive to finite size corrections to verify this scaling numerically, as we now explain.

We note, that the definition of E_T in terms of Δ_2 , while conceptually straightforward, is prone to significant finite size effects. This is because the shape of $f^2(\omega)$ changes significantly for small L , and therefore the plateau region has to be either defined with a very large “tolerance” ϵ or ΔE_T can change drastically as L increases. We illustrate the problem in Fig. S2, where Δ_2/d (essentially $\int_0^{\Delta E} f^2(\omega) d\omega / \Delta E$) is shown as a function of ΔE for different L . Finite size effects in the definition of ΔE_T is one of the main factors complicating finite scaling analysis of $\Delta E_U / \Delta E_T$.

Finally, we define ΔE_U – the central concept introduced in this paper – as the scale marking the onset of emergent unitary symmetry. Namely we require that for $\Delta E \leq \Delta E_U$ free cumulants scale as outlined in (S18). Again, we can introduce arbitrary small ϵ and define an energy scale $\Delta E_U^{(k)}$ as the point of deviation from the unitary invariance-imposed behavior for Δ_k , cf. (S32),

$$\left| \frac{\Delta_k}{a_k (\Delta E)^{k-1}} - 1 \right|_{\Delta E_U^{(k)}} = \epsilon, \quad (\text{S34})$$

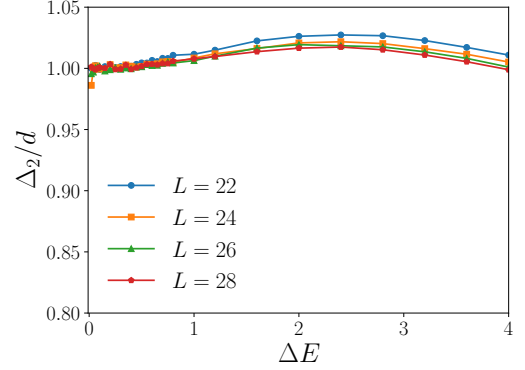


FIG. S2. Δ_2/d versus ΔE for the operator $\mathcal{A}_{q=\frac{1}{2}}$. This operator, in the large system size limit, should have L -independent thermalization time. This behavior is difficult to observe from the available data for Δ_2 . The data confirms, that for small ΔE the ratio Δ_2/d is approximately constant (the plateau of $f^2(\omega)$). Now, if we define ΔE_T as the point where Δ_2/d deviates, say by 1%, from the constant value, the approximate numerical value will be $\Delta E_T \approx 0.3$. But since the curve of (Δ_2/d) changes its overall shape for growing L , it is conceivable that for large L the “plateau” region will extend to much large values of order $\Delta E_T \approx 1 - 1.5$.

where $a_k (\Delta E)^{k-1}$ is the best fit for Δ_k for small ΔE . As above, as the system size grows, we can neglect nonlinearities of the energy spectrum density distinguishing $(\Delta E)^{k-1}$ from d^{k-1} . We notice that in all cases considered, $\Delta E_U^{(l)} \leq \Delta E_U^{(k)}$ for $l < k$. Therefore we can equivalently say that for $\Delta E \leq \Delta E_U^{(k)}$, all cumulants Δ_l with $l \leq k$ deviate from Eq. (S18) by not more than some ϵ .

With this definition we readily find $\Delta E_U^{(2)} = \Delta E_T$. In our numerical analysis we defined $\Delta E_U = \Delta E_U^{(4)}$ and saw that in most cases $\Delta E_U^{(6)} \approx \Delta E_U^{(4)} \ll \Delta E_U^{(2)} = \Delta E_T$. An interesting question is to understand the scaling of $\Delta E_U^{(k)}$ for $k \gg 1$. To this end, we introduce one more scale ΔE_{GUE} which marks the onset of Gaussian RMT universality. Gaussian RMT is characterized by vanishing higher free cumulants, $\Delta_k = 0$, except for $k = 2$. It is natural thus to define $\Delta E_{GUE}^{(k)}$, similarly to (S34), as a maximal value of ΔE within which all higher moments, properly normalized, plunge below some ϵ ,

$$\left| \frac{\Delta_k}{(\Delta_2)^{k/2}} \right|_{\Delta E_{GUE}^{(k)}} = \epsilon. \quad (\text{S35})$$

So far the operator exhibits emergent unitary symmetry, (S18) predicts

$$\frac{\Delta_k}{(\Delta_2)^{k/2}} \sim \left(\frac{d(\Delta E)}{d(\Delta E_U^{(k)})} \right)^{\frac{k}{2}-1} \rightarrow 0, \quad (\text{S36})$$

for small ΔE . Thus, we immediately conclude that for any small but fixed ϵ , Gaussian RMT scale $\Delta E_{GUE}^{(k)}$ will

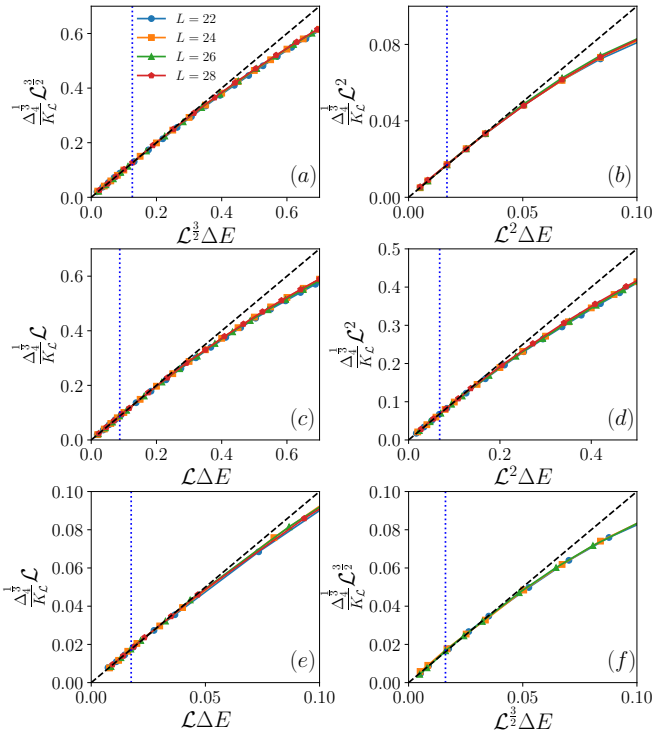


FIG. S3. $\frac{\Delta_k^{1/3}}{K_L^{1/3}} \mathcal{L}^p$ versus $\mathcal{L}^p \Delta E$ with the best fit values of K_L and p to achieve L -independence (best data collapse) for (a) $\mathcal{A}_{q=1/2}$; (b) $\mathcal{A}_{q=1}$; (c) $\mathcal{B}_{q=1/2}$; (d) $\mathcal{B}_{q=1}$; (e) $\mathcal{B}_{q=0}$ and (f) local energy operator \mathcal{A} (S40). Here $\mathcal{L} = L/24$ and we use $p = n/2$ with integer n as a tuning parameter. As a guide to the eye, inclined dashed black lines and vertical dotted blue lines indicate theoretical behavior $\Delta_k^{\frac{1}{k-1}} \propto \Delta E$ and the approximate location of ΔE_U , respectively.

be (much) smaller, but not parametrically (in terms of system-size dependence) smaller than $\Delta E_U^{(k)}$.

This conclusion, combined with the result of [9] suggests a non-trivial scaling hierarchy. Indeed, by considering thermalization of the density-wave operators (of the type introduced in Eq. (11) in the main text) in 1D systems, and assuming they are coupled to conserved quantity with the sub-ballistic (e.g. diffusive) transport, Ref. [9] imposed a bound on the ΔE_{GUE} scale,

$$\Delta E_{GUE} \lesssim \Delta E_T / L. \quad (\text{S37})$$

This scale has a simple physical interpretation of inverse timescale when the expectation value of \mathcal{O} in some initial out-of-equilibrium state $|\Psi\rangle$ will become of order of quantum fluctuations,

$$\langle \Psi | \mathcal{O}(t) | \Psi \rangle \approx e^{-\Delta E_T t} \sim e^{-S/2}. \quad (\text{S38})$$

The bound (S37) is based on the property of Gaussian RMT that the largest eigenvalue of the microcanonically truncated operator will grow with ΔE as $\sqrt{\Delta E}$. (This is the same as the size of Wigner's semicircle distribution

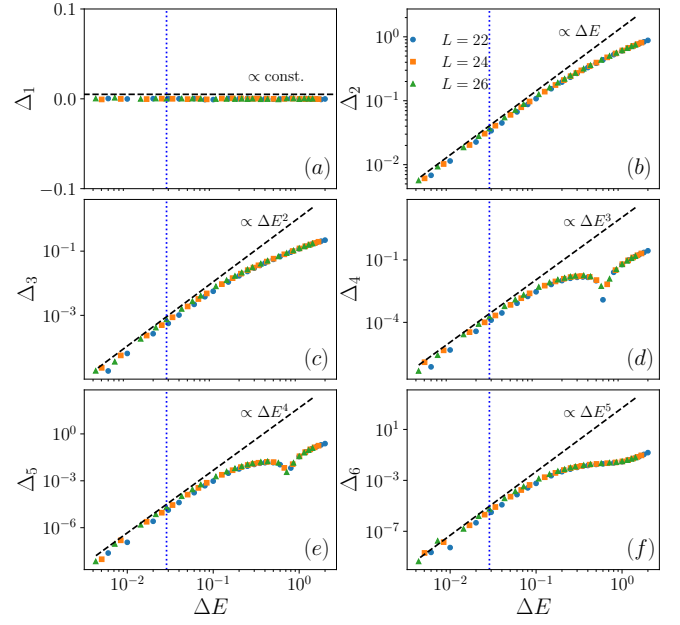


FIG. S4. Free cumulants Δ_k versus ΔE for local operator \mathcal{A} . As a guide to the eye, inclined dashed lines (black) and vertical dotted lines (blue) indicate theoretically predicted slope $\ln \Delta_k = (k-1) \ln \Delta E + \text{const.}$, and an approximate location of ΔE_U , respectively.

being proportional to square root of the matrix size \sqrt{d} .) This behavior is guaranteed, provided Δ_2^k gives leading contribution to \mathcal{M}_{2k} (S9), or $\Delta_{2k}/(\Delta_2)^k \ll 1$ for $k \gg 1$. In other words, for $k \gg 1$, $\Delta E_{GUE}^{(k)}$ obeys (S37). Combining all together we find $\Delta E_{GUE}^{(k)} \ll \Delta E_U^{(k)}$ while both scale with L as

$$\Delta E_T / L \sim \frac{q^2}{L^3}, \quad (\text{S39})$$

and thus *parametrically* smaller than ΔE_T .

We emphasize, the system size scaling (S39) should apply to $\Delta E_{GUE}^{(k)}$, $\Delta E_U^{(k)}$ with $k \gg 1$, while in our numerical analysis we used $k = 4$. We leave open the question of how $\Delta E_U^{(k)} / \Delta E_U^{(l)}$ would scale with the system-size when $k \gg l$. Elucidating this question would be necessary to confirm the hierarchical behavior $\Delta E_{GUE} \ll \Delta E_U \ll \Delta E_T$ introduced in the main text.

Additional numerical results

System size dependence of ΔE_U . Numerically, the procedure to determine ΔE_U from Eq. (S34) is not very accurate. To study L dependence of ΔE_U we employ a different approach. Considering an operator of interest, we try to find two tuning parameters K_L and p such that the curves of $\frac{\Delta_k^{1/3} L^p}{K_L}$ as a function of $L^p \Delta E$ for different L would approximately be L -independent. We do this in two steps. We first consider $\Delta_{4/3}$, which grows linearly for

small ΔE , and find K_L^{-1} such that for very small ΔE , $K_L^{-1}\Delta_4^{\frac{1}{3}} \approx \Delta E$. Next we find a tuning parameter p to achieve best possible data collapse (L -independence) of $\frac{\Delta_4^{\frac{1}{3}}}{K_L}L^p$ as a function of $L^p\Delta E$. We choose p in the form $p = \frac{n}{2}$ with integer n . For convenience instead of L we use $\mathcal{L} = L/24$ and plot $\frac{\Delta_4^{\frac{1}{3}}}{K_{\mathcal{L}}}L^p$ as a function of $\mathcal{L}^p\Delta E$. The results are shown in in Fig. S3, where we find p to be positive for all operators considered. This suggests $\Delta E_U \sim L^{-p}$ scaling with positive p .

Our results suggest that $\Delta E_U \propto \mathcal{L}^{-p}$ with $p \geq 0$, but the precise value of p is dependent on the observable of interest. While a perfect data collapse is difficult to achieve for most observables, the precise finite-size scaling of ΔE_U remains unclear. This should not come as a surprise, as the system sizes $L = 22, \dots, 28$ are likely still too small to observe the asymptotic scaling regime.

Local operators. Next we consider a local energy density operator ,

$$\mathcal{A} = \frac{\hbar}{2}(\sigma_x^1 + \sigma_x^2) + \frac{g}{2}(\sigma_z^1 + \sigma_z^2) + J\sigma_z^1\sigma_z^2. \quad (\text{S40})$$

Numerical results are show in Fig. S4. Similar to the density wave operator, apart from the deviations at extremely small ΔE , $\Delta_k \propto \Delta E^{k-1}$ behavior is observed below certain energy scale, indicating emergence of unitary symmetry at $\Delta E \leq \Delta E_U$.

Finally in Fig. S5, we study another local operator

$$\mathcal{B} = \hbar\sigma_z^1 - g\sigma_x^1. \quad (\text{S41})$$

Similarly, $\Delta_k \propto \Delta E^{k-1}$ behavior emerges within a sufficiently small energy window.

Indicator of distance to GUE. For an operator exhibiting unitary symmetry, Eq. (S19) implies $\Delta_k/(\Delta_2)^{k/2} = \lambda_k/\lambda_2^{k/2} \Delta E^{k/2-1} \rightarrow 0$ when $\Delta E \rightarrow 0$, which indicates emergence of GUE behavior at sufficiently small ΔE . Therefore, the factor $\lambda_k/\lambda_2^{k/2}$ can be regarded as an indicator of distance to GUE at given ΔE . In Table. I we report the (approximate) values of $\mu_k = (\lambda_2^{k/2}/\lambda_k)^{1/(k/2-1)}$ for several operators and different system sizes. Values of μ_k , which have dimension of energy, would indicate the scale where deviation of k -th cumulant from the GUE is still very significant. The observed values of μ_4 are of order 0.1 – 1, highlighting that GUE is only applicable at scales $\Delta E \ll 1$.

Integrable system. Complementary to chaotic systems, we also consider an integrable model, an Ising model with inhomogeneous transverse field

$$H = \sum_{\ell=1}^L (g\sigma_x^\ell + J\sigma_z^\ell\sigma_z^{\ell+1}) + h_1\sigma_x^{\lfloor \frac{L}{3} \rfloor} + h_2\sigma_x^{\lfloor \frac{2L}{3} \rfloor}, \quad (\text{S42})$$

where $J = 1, g = \frac{\sqrt{5}}{2}, h_1 \simeq 0.062, h_2 \simeq -0.09$. The two defect terms are added to break the translational and

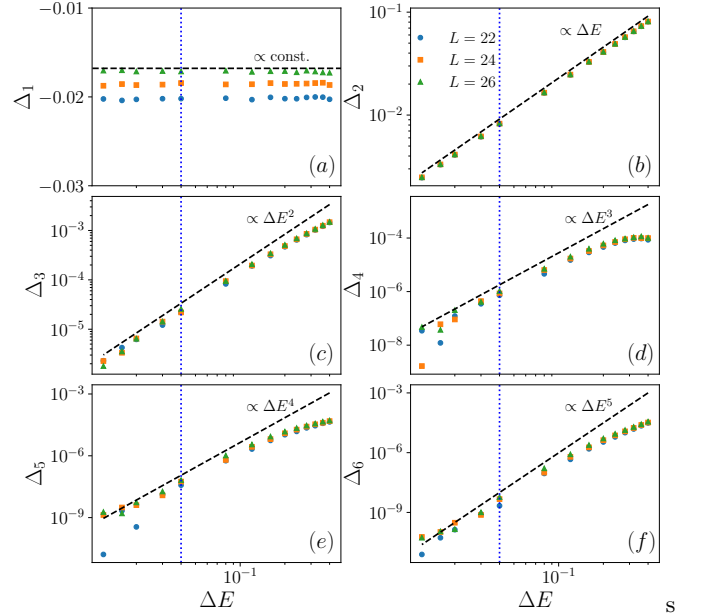


FIG. S5. Similar to Fig. S4, the results for local operator \mathcal{B} .

	μ_4		μ_4
$\mathcal{A}_{L/2}(L = 24)$	1.0	$\mathcal{B}_{L/2}(L = 24)$	0.8
$\mathcal{A}_{L/2}(L = 28)$	0.9	$\mathcal{B}_{L/2}(L = 28)$	0.7
$\mathcal{A}_1(L = 24)$	0.1	$\mathcal{B}_1(L = 24)$	0.6
$\mathcal{A}_1(L = 28)$	0.08	$\mathcal{B}_1(L = 28)$	0.5

TABLE I. List of approximated value of μ_4 for different operators and different system sizes.

reflection symmetries of H . The observables considered are energy density wave operators

$$\mathcal{A}_q = \frac{1}{\sqrt{L}} \sum_{\ell=1}^L \cos\left(\frac{2\pi}{L}q\ell\right)\mathcal{A}^\ell, \quad (\text{S43})$$

where

$$\mathcal{A}^\ell = \frac{\hbar}{2}(\sigma_x^\ell + \sigma_x^{\ell+1}) + J\sigma_z^\ell\sigma_z^\ell. \quad (\text{S44})$$

In contrast to chaotic cases, deviation from the $\Delta_k \propto \Delta E^{k-1}$ behavior is clearly visible in Fig. S6, indicating that unitary symmetry does not emerge even at very small scales.

Details of the numerical method

The key idea of our numerical approach is the expansion of projector operator $P_{\Delta E} = \sum_{|E_m - E_0| < \Delta E/2} |m\rangle\langle m|$ in terms of Chebyshev polynomials of the Hamiltonian given, see Eq. (S52) in the main text. In this section, we are going to explain the numerical method in more detail.

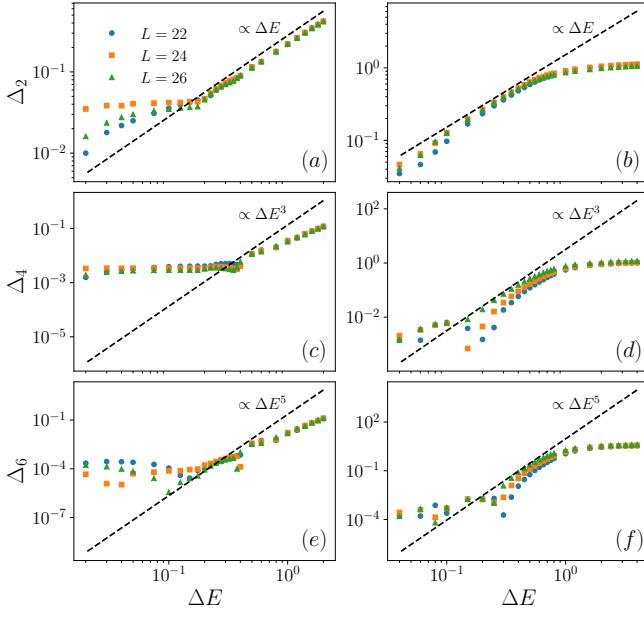


FIG. S6. Even cumulants Δ_k for $k = 2, 4, 6$ as a function of ΔE in the (integrable) transverse field Ising model (S42), for the density-wave operator \mathcal{A}_q with the wave-number $q = \frac{L}{2}$ (panels [(a),(c),(e)] and with $q = 1$ (panels [(b),(d),(f)]). Data is shown for different system sizes $L = 22, 24, 26$. As a guide to the eye, inclined dashed black lines indicate the slope $\ln \Delta_k = (k - 1) \ln \Delta E + \text{const}$.

In the eigenbasis, $P_{\Delta E}$ can be written as,

$$P_{\Delta E} = \sum_m P_{\Delta E}(E_m) |m\rangle \langle m|, \quad (\text{S45})$$

$$P_{\Delta E}(E) = \text{rect} \left(\frac{E - E_0}{\Delta E} \right), \quad (\text{S46})$$

where $\text{rect}(x)$ indicates the rectangular function defined as,

$$\text{rect}(x) = \begin{cases} 0 & \text{if } |x| \geq \frac{1}{2} \\ 1 & \text{if } |x| < \frac{1}{2} \end{cases}. \quad (\text{S47})$$

The rectangular function can be expanded in terms of Chebyshev polynomials of the first kind (denoted by $T_k(x)$),

$$P_{\Delta E}(E) = \sum_{k=0}^{\infty} C_k T_k \left(\frac{E - b}{a} \right), \quad (\text{S48})$$

where $a = (E_{\max} - E_{\min})/2$, $b = (E_{\max} + E_{\min})/2$. The coefficients C_k are written as

$$C_0 = \frac{1}{\pi} \left[\arcsin \left(\frac{\frac{\Delta E}{2} + b - E_0}{a} \right) - \arcsin \left(\frac{-\frac{\Delta E}{2} + b - E_0}{a} \right) \right], \quad (\text{S49})$$

and

$$C_k (k \geq 1) = \frac{2(-1)^{k+1}}{\pi k} \left[\sin \left(k \arccos \left(\frac{\frac{\Delta E}{2} + b - E_0}{a} \right) \right) - \sin \left(k \arccos \left(\frac{-\frac{\Delta E}{2} + b - E_0}{a} \right) \right) \right]. \quad (\text{S50})$$

In practice, the infinite series in Eq. (S48) needs to be truncated to finite order N_{tr} ,

$$P_{\Delta E}(E) \simeq \sum_{k=0}^{N_{\text{tr}}} C_k T_k \left(\frac{E - b}{a} \right). \quad (\text{S51})$$

In the following, we denote N_{tr} by N for simplicity. $P_{\Delta E}$ finally can be approximated as

$$P_{\Delta E} \simeq P_{\Delta E}^{(N)} \equiv \sum_{k=0}^N C_k T_k \left(\frac{H - b}{a} \right). \quad (\text{S52})$$

Applying the above equation to a Gaussian random state

$$|\psi\rangle = \sum_{i=1}^D c_i |i\rangle, \quad (\text{S53})$$

where c_i is a Gaussian random number and $|i\rangle$ denote the computational basis, the k -th moment of an operator \mathcal{O} can be approximated by relying on quantum typicality,

$$\mathcal{M}_k \simeq \frac{\langle \psi | (P_{\Delta E}^{(N)} \mathcal{O} P_{\Delta E}^{(N)})^k | \psi \rangle}{\langle \psi | P_{\Delta E}^{(N)} | \psi \rangle}. \quad (\text{S54})$$

Moreover, making use of $(P_{\Delta E}^{(N)})^2 \simeq P_{\Delta E}^{(N)}$, Eq. (S54) is simplified as

$$\mathcal{M}_k \simeq \mathcal{M}_k^{\text{typ}} \equiv \frac{\langle \psi | P_{\Delta E}^{(N)} (\mathcal{O} P_{\Delta E}^{(N)})^k | \psi \rangle}{\langle \psi | P_{\Delta E}^{(N)} | \psi \rangle}, \quad (\text{S55})$$

where one only needs to apply the energy filter $P_{\Delta E}^{(N)}$ for $k+1$ times, instead of $2k$ times in the original expression (S54). In the numerical simulations, to further reduce statistical errors, an additional average is taken over N_{typ} different realization of random state,

$$\overline{\mathcal{M}_k^{\text{typ}}} = \frac{1}{N_{\text{typ}}} \sum_{n=1}^{N_{\text{typ}}} \frac{\langle \psi_n | P_{\Delta E}^{(N)} (\mathcal{O} P_{\Delta E}^{(N)})^k | \psi_n \rangle}{\langle \psi_n | P_{\Delta E}^{(N)} | \psi_n \rangle}. \quad (\text{S56})$$

where $|\psi_n\rangle$ indicates an individual realization of a Gaussian random state. The Chebyshev expansion becomes more accurate if one increases the number of terms in the expansion N , but the simulation time is proportional to N , hence larger N will result in a longer simulation time. In our numerical simulations $N = 100a \frac{2\pi}{\Delta E}$ which is found to yield high accuracy of results.

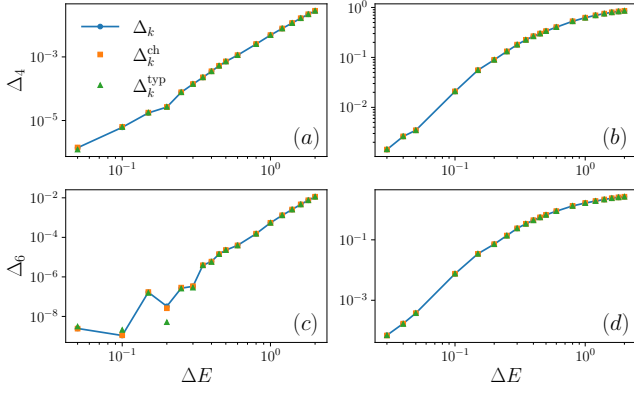


FIG. S7. Comparison of Δ_k^{typ} (green triangle, averaged over 2^{12} random states), Δ_k^{ch} (orange square) and Δ_k (blue circle with solid line, calculated by ED) for operator: [(a) (c)] $\mathcal{A}_{q=\frac{1}{2}}$ and [(b) (d)] $\mathcal{A}_{q=1}$ for system size $L = 16$.

Error analysis

In this section, we perform an error analysis of our typicality-based numerical method. The total error in our approach comes from two different sources: (i) a truncation error ε_{tr} [due to the finite order N in the Chebyshev expansion (S52)], and (ii) a typicality error ε_{typ} [due to approximating the trace by a random state in Eq. (S54)]. The typicality error ε_{typ} is easy to estimate. It scales as $\varepsilon_{\text{typ}} \sim (N_{\text{typ}}d)^{-1/2}$, where d is the number of states in the energy window. In the numerical simulations, N_{typ} is chosen according to the system size, $N_{\text{typ}} \propto 2^{-L}$, which then assures similar accuracy for different L . More precisely, the typicality error for the approximation of \mathcal{M}_k is given by

$$\varepsilon_{\text{typ}}(\mathcal{M}_k) = \sqrt{\frac{\mathcal{M}_{2k} - \mathcal{M}_k^2}{N_{\text{typ}}d}}. \quad (\text{S57})$$

The relative (typicality) error is given by

$$\frac{\varepsilon_{\text{typ}}(\mathcal{M}_k)}{|\mathcal{M}_k|} = \sqrt{\frac{\mathcal{M}_{2k} - \mathcal{M}_k^2}{\mathcal{M}_k^2}} \frac{1}{\sqrt{N_{\text{typ}}d}}. \quad (\text{S58})$$

We will readily see that it depends on the order k . To estimate the relative error of even moments, let's consider the case where all odd moments vanish. It is known that if an operator can be described by a GOE random matrix, one has

$$\mathcal{M}_{2k} = \Lambda_k (\mathcal{M}_2)^k, \quad (\text{S59})$$

where $\Lambda_k = \frac{(2k)!}{(k+1)!k!}$ is the Catalan number. Within a small energy window $\Delta E \ll \Delta E_U$, k -th cumulant decays as $\Delta_k \propto (\Delta E/\Delta E_U)^{k-1}$. In this case, Eq. (S59) holds approximately, at least with respect to scaling. There-

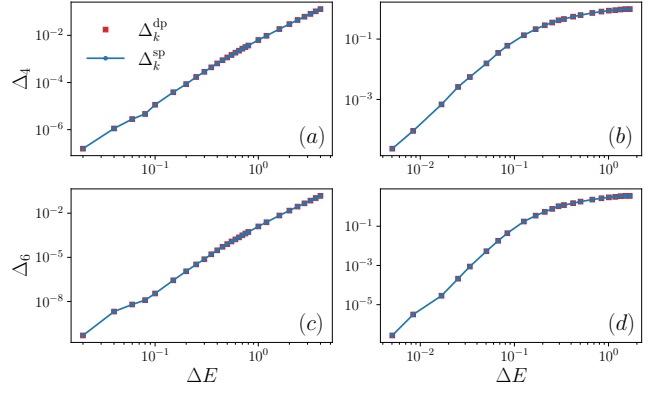


FIG. S8. Comparison of result of Δ_k from single precision Δ_k^{sp} (blue circle) and double precision Δ_k^{dp} (red square) simulations, for operator: [(a) (c)] $\mathcal{A}_{q=\frac{L}{2}}$ and [(b) (d)] $\mathcal{A}_{q=1}$ for system size $L = 24$. The result is obtained from a same random state.

fore, one has

$$\frac{\mathcal{M}_{2k} - \mathcal{M}_k^2}{\mathcal{M}_k^2} \sim \frac{\Lambda_k}{\Lambda_{\frac{k}{2}}} \sim k^{\frac{3}{2}}, \quad \text{for even } k \gg 2. \quad (\text{S60})$$

As a result one has the following estimation for even moments

$$\frac{\varepsilon_{\text{typ}}(\mathcal{M}_k)}{|\mathcal{M}_k|} \sim k^{\frac{3}{4}} \frac{1}{\sqrt{N_{\text{typ}}d}}, \quad (\text{S61})$$

indicating that the relative error of \mathcal{M}_k increases as a power law in k . For the density-wave operators with non-zero wave number, odd moments approximately vanish. So in our numerical simulation, we neglect all the odd moments and only even moments are considered. For all other operators, for which the odd moments are not negligibly small, the ratio $\frac{\mathcal{M}_{2k} - \mathcal{M}_k^2}{\mathcal{M}_k^2}$ is operator-dependent.

Usually we expect that $\frac{\mathcal{M}_{2k} - \mathcal{M}_k^2}{\mathcal{M}_k^2}$ increase with k , which leads to a larger relative error for higher moments. It should be mentioned here that, as free cumulants Δ_k are calculated by making use of moments \mathcal{M}_k , their relative error are in general larger than that of \mathcal{M}_k .

The truncation error ε_{tr} depends on the number of Chebyshev polynomials we keep in the expansion of Eq. (S52). Different from the typicality error, an analytical expression of truncation error is very hard to derive. We try to estimate ε_{tr} numerically instead. To this end, we consider

$$\mathcal{M}_k^{\text{ch}} \equiv \frac{\text{Tr} \left[P_{\Delta E}^{(N)} (OP_{\Delta E}^{(N)})^k \right]}{\text{Tr} \left[P_{\Delta E}^{(N)} \right]}. \quad (\text{S62})$$

It can be easily seen that $\mathcal{M}_k^{\text{ch}} \rightarrow \mathcal{M}_k$ for $N \rightarrow \infty$ and $\overline{\mathcal{M}_k^{\text{typ}}} \rightarrow \mathcal{M}_k^{\text{ch}}$ if the Hilbert-space dimension is sufficiently large or if the results are averaged over many

realizations of random state. Here $\overline{\mathcal{M}_k^{\text{typ}}}$ indicates that the trace is approximated by random states. We denote the cumulants calculated by $\overline{\mathcal{M}_k^{\text{typ}}}$ and $\mathcal{M}_k^{\text{ch}}$ as Δ_k^{typ} and Δ_k^{ch} , respectively. The error ε_{typ} and ε_{tr} can be probed by

$$\varepsilon_{\text{tr}} \propto |\Delta_k^{\text{ch}} - \Delta_k|, \quad \varepsilon_{\text{typ}} \propto |\Delta_k^{\text{ch}} - \Delta_k^{\text{typ}}|. \quad (\text{S63})$$

We compare Δ_k^{typ} , Δ_k^{ch} and Δ_k for system size $L = 16$ in Fig. S7. For the operators considered, a neat agreement between Δ_k^{ch} and Δ_k can be seen, indicating a small

truncation error ε_{tr} . Δ_k^{typ} (calculated by averaging over 2^{12} random states) also remains very close to Δ_k^{ch} for almost all ΔE , indicating a small typicality error ε_{typ} . Deviations can be observed for $\Delta E \rightarrow 0$, especially for Δ_6 of $\mathcal{A}_{q=\frac{L}{2}}$ [Fig. S7 (c)] when the number of states within the energy window plunges below $d \lesssim 1000$.

It should be mentioned here that all our numerical simulations with the typicality-based method are done in single precision. The accuracy of single precision simulation is checked in several observables (see Fig. S8), where we find that the difference between results from single and double precision simulations are neglectably small.